Modulation of the photochromic properties of TPE and other tetrasubstituted olefins by the "amino conjugation effect": a quantitative study

Jean Rouillon,[*a,b] Chantal Andraud[a] and Cyrille Monnereau[a]

a/ Univ Lyon, Ecole Normale Supérieure de Lyon, Laboratoire de Chimie, CNRS UMR 5182, 69342 Lyon, France
b/ Department of Chemistry and Chemical Engineering, Chalmers University of Technology, Kemigården 4, 412 96 Göteborg, Sweden.

Abstract

Tetraphenylethylene (TPE) derivatives have been a key building block in the development of solid-state fluorophores with tunable emission wavelength and large quantum efficiencies. Recent literature has brought an array of evidence that rotation around the central C=C bond constitutes main route of deexcitation in solution, and that its restriction in solid-state leads to aggregation-induced emission (AIE) in this family of derivatives. However, the influence of substitution on the dynamics of TPEs in solution has so far received little attention, probably because of the difficulty in efficiently separating (E) and (Z) isomers. Here we report the photophysical properties in solution of extended stereopure TPE derivatives. The introduction of triphenylamine (TPA) substituent results in differences in the spectral properties between the (E) and (Z) isomers, thereby allowing modulation of the photostationary state (PSS) and thus switching in the equilibrium between these two forms depending on the irradiation wavelength. Importantly, we show that this photochromism is observed with a very marked decrease in the photoisomerization quantum yields (Φ_{iso}) of TPE-TPA, compared to non-extended TPE derivatives, which we attribute to the so called "amino conjugation effect" already reported for several stilbene derivatives. As a generalization of this mechanism, we show that TPA substitution provides similar effect on other stilbenoid derivatives. These results provide important new insight into the photophysics of electron donor substituted TPEs, and their possible use as photochromic materials.

Introduction

Extended aromatic olefins are the most widely studied class of organic dyes, and the range of topics in which they are involved is constantly expanding.[1–4] Particular emphasis has been placed on the photochemistry and photophysics of aromatic olefins, both in solution and in the aggregated state.[5–7] Within this family of compounds, stilbenes and related analogues have been particularly studied due to the variety of processes accessible in their excited state, such as E/Z photoisomerization and the photocyclization reactions.[8] Among the stilbenoids, tetraphenylethylene (TPE) derivatives have been, , a comparatively overlooked class of materials in this regard.[9–13] Indeed, although their solid state properties have been widely explored, making them key components in the molecular engineering of solid state fluorophores or AIEgens,[14,15] their photochemistry in solution has long remained comparatively unexplored (Fig. 1a).

Recently, an increasing number of studies using a variety of steady-state and time-resolved spectroscopies coupled with theoretical calculations have painted a rather complex landscape of the excited state of TPE derivatives, giving rise to sometimes conflicting conclusions about their photochemical evolution in solution.[12,13,16–19] We have recently reported for the first time a numerical estimation of the photoisomerization (Φ_{iso}) and photocyclization (Φ_c) quantum yields of fluorine- and methoxy-substituted derivatives TPE-F and TPE-OMe respectively (Fig. 1a).[20] This was achieved using a tailored actinometric NMR protocol.[21] With this protocol in hand, it was possible to provide conclusive evidence that rotation around the central double bond, i.e. photoisomerization, is an almost exclusive deactivation pathway of the TPE excited state in solution, in the absence of oxygen. Chemically irreversible photocyclization, although minor in terms of quantum yields (0.05), plays a role in the photochemical evolution of the system upon prolonged irradiation of aerated solutions.

This study remained however limited to small TPE derivatives with simple substitution patterns, having little influence on the electronic properties of the π-conjugated backbone.
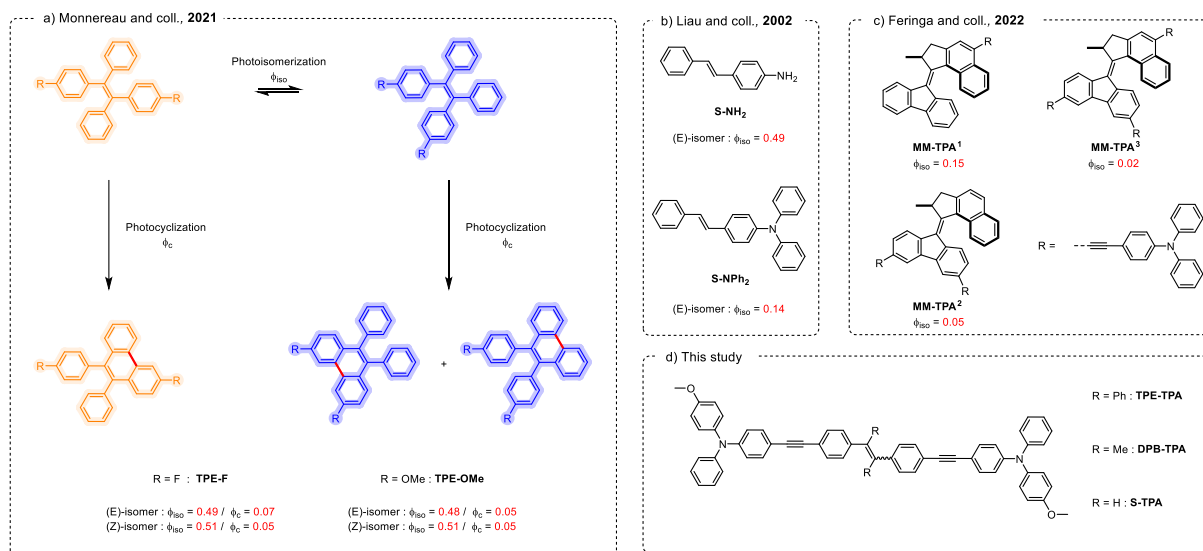
Fig. 1 a) Photochemical pathways involved for TPE-OMe and TPE-F studied by Monnereau and coll.[20]; Photoisomerization quantum yields of derivatives developed by b) by Liau and coll.[22] and c) Feringa and coll.[23]; d) Structures of TPE-TPA, DPB-TPA and S-TPA studied in the present article.

In the case of stilbenes, the influence of the introduction of electroactive substituents (electron donating or withdrawing) on the photochemical processes in general, and photoisomerization in particular, has been extensively studied.[8] In particular, the effect of N-phenylamino, referred to as "amino conjugation effect" substitution on the para-position of stilbene derivatives has clearly been demonstrated in a recent study by Liau and coll. (Fig. 1b).[22] In this work, it was shown that such substitution significantly alters the photophysics of the resulting chromophore: stilbenoids usually has a high photoisomerization quantum yield (Φ_{iso} = 0.49 for S-NH$_2$ in hexane) which is detrimental to their fluorescence properties (Φ_f = 0.03 for S-NH$_2$ in hexane). With the amino conjugation effect, a significant decrease in the photoisomerization quantum yield was observed (Φ_{iso} = 0.14 for S-NPh2 in hexane), while the fluorescence quantum yield Φ_f in solution (Φ_f = 0.57 for S-NPh2 in hexane) was increased to a similar extent (Fig. 1).

It has been proposed that the charge transfer induced by the N-phenyl substitution leads to a better stabilization of the planar S1 state of the (E), away from the orthogonal twisted form, largely suppressing the conical intersection pathway at the origin of photoisomerization process,[13] and making the rotational energy barrier around the central C=C bond higher for the N-phenylamine derivative compared to its amino equivalent. Thus, the amino conjugation effect reduces the photoisomerization process in favor of luminescence. Very recently, a similar effect was also described by Feringa and coll. on their molecular motors MM-TPA (Fig. 1c):[23] adding TPA substituents, conjugated to the stiff-stilbene core through a triple bond, leads to a strong decrease of the Φ_{iso} yields (Φ_{iso}(MM-TPA[1]) = 0.15 ; Φ_{iso}(MM-TPA[2]) = 0.05 ; Φ_{iso}(MM-TPA[3]) = 0.02).

To date, however, generalization of these conclusions to more diversified classes of stilbenoids, including TPE derivatives that have gained a lot of attention for their abovementioned importance in solid state emissive material sciences, are still lacking. A possible explanation to this fact may rely in the difficult separation of the (E) and (Z) isomers of TPE derivatives,[10] which adds to the inherently non-trivial measurements of Φ_{iso} and Φ_c (*vide supra*). In a previous study,[24] we introduced a new method for the separation of the (E) and (Z) isomers of extended triphenylamine (TPA) substituted TPEs by means of chiral preparative HPLC (Fig. 1d).

In the present report, we take advantage of these preliminary results, which allowed us to get pure TPE-TPA (E) and (Z) isomers and then to initiate a study of their photochromic properties and the determination of their associated photoisomerization quantum yields Φ_{iso}. As anticipated, we show that the significant TPA substitution gives rise to a marked intramolecular charge transfer character to the lowest energy electronic transition, resulting in significant spectroscopic differences between (E) and (Z) isomers. We show, depending on the irradiation wavelength, that we can achieve a control over (E) and (Z) isomers ratio of TPE-TPA, which constitutes the basis of a photochromic system. In addition, the calculated Φ_{iso} yields of TPE-TPA and other olefinic compounds, DPB-TPA and S-TPA, highlights that the "amino conjugation effect", already reported on other stilbenoid derivatives[22,23] also applies here, which results in a marked slow-down of the photoisomerization kinetics. Although detrimental for a potential use as a photochromic molecule/molecular rotor, this effect contributes in stabilizing the (E) or (Z) form of such elongated TPE derivatives, with potential benefits for such applications as one or two-photon fluorescence bioimaging, for which we recently brought proof of concepts.[24,25]

Results and discussion

The spectroscopic properties of the (E) and (Z) isomers of TPE-TPA have been studied in solution in chloroform (Fig. 2a). As a first remark, it is important to note that the vast majority of TPE derivatives reported in the literature show truly little influence of their stereo configuration on their absorption maxima (cf. Table S8). However, in the case of TPE-TPA, while the absorption band of the (Z) isomer peaks at 367 nm, (E) isomer shows a maximum at 376 nm. To our knowledge, this energy difference of 674 cm^{-1} is the largest difference between TPE isomers reported to date: we were able to rationalize this difference in a previous report based on TD-DFT modelling of the excited states of both stereoisomers.[24] Indeed, calculations on the first two transitions showed that only the lower energy $S_0 \rightarrow S_1$ transition is allowed in the (E) isomer as a consequence of the quadrupolar nature of the molecule, whereas the higher energy $S_0 \rightarrow S_2$ transition, although not exclusive, is largely favored in the dipolar (Z) isomer, resulting in a noticeable difference in the absorption maxima and overall band shape for the two isomers.

The green curve in Fig. 2a represents the difference in absorbance between the (E) and (Z) isomers. This curve highlights three characteristic wavelengths (highlighted with red dots): (i) 350 nm, where the difference in absorbance between the (Z) and (E) isomers is greatest, in favor of (Z) (ca. 20%); (ii) 350 nm, where the difference in absorbance between the (Z) and (E) isomers is greatest, in favor of (E) (ca. +20%); (iii) the isobestic point at 372 nm.

This disparity led us to investigate the photochromic properties of the TPE-TPA isomers, i.e., the possibility of tuning their E/Z ratio photochemically by varying the excitation wavelength (Fig. 2b).
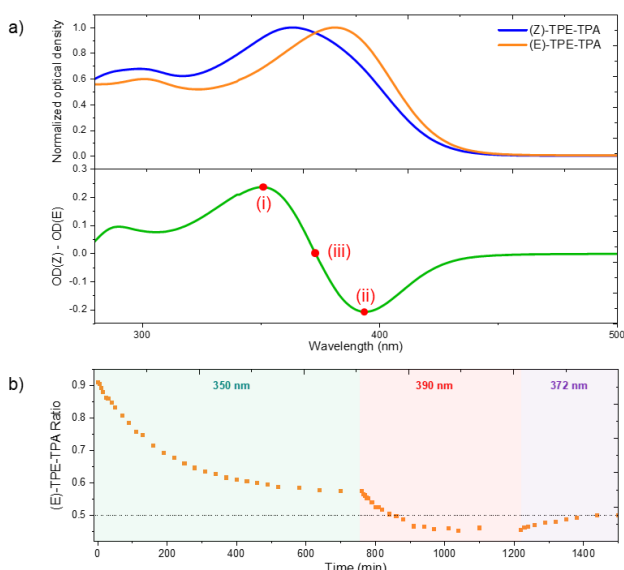

Fig. 2 a) Absorption spectra in chloroform of (Z) and (E) isomers of **TPE-TPA** (blue and yellow respectively) and the difference of the absorption of (Z) with (E) isomer (green) with characteristic wavelength indicated by red dots b) Photoisomerization kinetic of **(E)-TPE-TPA**. Colored zones indicate the irradiation wavelengths during the associated period and black horizontal line indicate the 1:1 E/Z ratio.
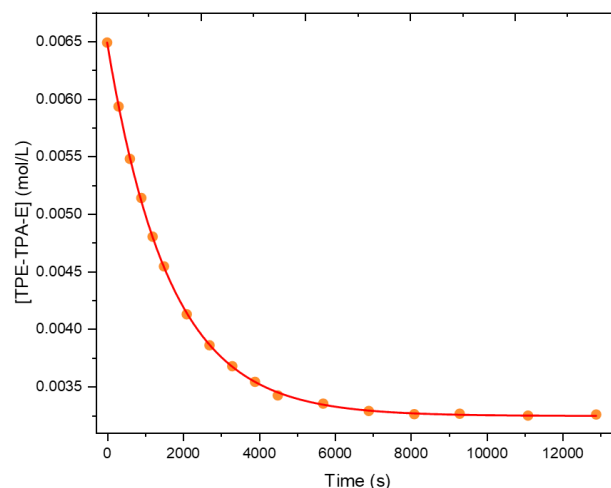

Fig. 3 Photoisomerization kinetics of (E)-TPE-TPA with in red, the exponential fit curve.

To monitor this process, a pure (E)-TPE-TPA solution was therefore irradiated at the different characteristic wavelengths mentioned above and the evolution of the E/Z ratio was determined at regular intervals by ^{1}H NMR (see detailed procedure in Supporting Information).

The first part of the kinetic curve (green area in Fig. 2) corresponds to the irradiation of the (E)-TPE-TPA solution at 350 nm. The kinetic profiles follow the expected mono-exponential decay associated with such a photoconversion process.[20] When the photostationary state (PSS) is reached after prolonged irradiation, an E/Z ratio of 58/42 is obtained, corresponding to a 16% excess of the (E) isomer over the (Z) isomer, close to the theoretical difference of 20% predicted by the absorption differences (Fig. 2b).

The second part of the curve (red area) corresponds to irradiation at the characteristic wavelength of 390 nm. In this case, the system evolves towards a photostationary equilibrium in which the (Z) isomer is predominant. The E/Z ratio at PSS is 46/54: the associated difference of 8% between the two isomers is smaller than that predicted by the differences in absorbance (again of the order of 20%).

Irradiation at the isosbestic point at 372 nm (purple region) of the mixture of isomers achieves the expected photoequilibrium with an E/Z ratio of 1:1. Overall, despite minor inconsistencies, the control of the photoequilibrium ratio based on the incident wavelength is consistent with the relative absorptions of each isomer: irradiation source that is not perfectly monochromatic may account for these differences.

Consequently, the introduction of TPA groups with high electronic impact on TPE induces a remarkable shift between the optical properties of the (E) and (Z) isomers. This difference allows the manipulation of the isomer ratio according to the excitation wavelength, enhancing the photochromism of the TPE derivatives. Thus, TPE derivatives can be used as photoswitches

Table 1 Photoisomerization quantum yields estimated in CDCl$_3$.

	$\Phi_{E \to Z}$	$\Phi_{Z \to E}$
TPE-TPA	0.08	0.09
DPB-TPA	0.04	0.06
S-TPA	0.18	-
TPE-F[a]	0.49	0.51
TPE-OMe[a]	0.48	0.51

a.   Data from ref.[20]

based on an E/Z isomerization mechanism as for azobenzenes, indigoids or stiff-stilbenes.[26]

To further assess the usefulness of TPE-TPA for potential photoswitching applications, the E/Z photoisomerization quantum yields were determined by irradiating stereopure solutions of the (E) and (Z) isomers at the isosbestic point (i.e. 372 nm) of both isomers, and fitting the resulting data according to our previously published protocol.[20,21]

The kinetics of the irradiation of (E)-TPE-TPA is shown in Fig. 3 (see details of the procedure and calculations in SI). During the irradiation process of these compounds, the formation of photocyclization or other

To extend this conclusion of the amino conjugation effect on AIEgens derivatives, the determination of Φ_{iso} yields was also performed on **DPB-TPA** isomers and **(E)-S-TPA**, which differ from **TPE-TPA** by the change of the two central phenyls by methyls or hydrogens respectively (Fig. 1). As illustrated in a previous report, all these designed compounds present interesting AIE properties.

Photoisomerization quantum efficiencies were first investigated for **DPB-TPA**, using a similar protocol as for TPE-TPA, and resulting data and fits are presented as supplementary material (Fig. S4-S6) Φ_{iso} yields are estimated to be 0.06 for the (Z) isomer and 0.04 for the (E) isomer (Table 1). These values are of the same order as those obtained for **TPE-TPA** and confirm that the solution excited state dynamics of these stilbenoids in solution is also governed mainly by this amino conjugation effect, which drastically limits their photoisomerization.

Finally, the photoisomerization quantum yield of **(E)-S-TPA** (Z counterpart is not synthetically accessible) was also evaluated, to Φ_{iso} = 0.18. This yield, higher compared to its equivalents **TPE-TPA** and **DPB-TPA**, remains well below that of related non-TPA substituted stilbenes, both tabulated (0.4-0.5)[27] or as reported by us (0.4) in previous studies using similar measurement protocol.[20] Moreover, the magnitude of decrease in photoisomerization efficiency appear consistent with that reported, also on stilbene (monosubstituted) by Liau and coll.: although separated from the stilbene core by a triple bond, the TPA groups modulate the photochemistry of these olefin derivatives.

photo-degradation products remained negligible under these conditions (< 5% detected by NMR after more than 3 hours irradiation). Thus, we report herein only the photoisomerization quantum yields. The experimental data (yellow points in Fig.3) could be fitted with good accuracy to a mono-exponential decay (red curve, Fig. 3). This allowed us to calculate Φ_{iso} yields of 0.08 for the (E) isomer and of 0.09 for the (Z) isomer (Fig. S1-S3 and Table S2). These Φ_{iso} yields are dramatically lowered when compared to those determined for the TPE-OMe and TPE-F derivatives, in the range of $\Phi_{iso} \approx$ 0.5 (Fig 1a., Table 1). This drastic decrease in Φ_{iso} yield agrees well, both qualitatively and quantitatively, with the previous conclusions of Liau and coll.[22] and Feringa and coll.[23] on other stilbenoid derivatives stabilized by to amino conjugation effect.

An interesting difference is however observed when comparing **TPE-TPA** and **DPB-TPA** on the one hand, and **S-TPA**, on the other. While, in the latter, the drop in photoisomerization quantum efficiency is accompanied by a significant improvement in luminescence efficiency (Φ_f = 0.65 for S-TPA vs Φ_f = 0.07[28] for unsubstituted stilbene), nothing comparable is observed in the former. Luminescence efficiency remains close to zero in this case, highlighting the existence of further nonradiative dissipative pathways, probably resulting from higher steric constraints around the double bond which favor twisting motions at the excited state.

Conclusions

In summary, we have studied the influence of TPA substitution on the photochromic properties of TPE derivatives. TPA group induces a charge transfer character to the electronic transition, which results in significant differences in the absorption properties of the (E) and (Z) **TPE-TPA** isomers. This difference, along with the possibility to induce E-Z photoisomerization at the excited state, allows controlled modulation of the E/Z ratio upon photoirradiation, depending on the incident excitation wavelength. This benefit of the introduction of TPA on the magnitude of photochromism between the (E) and (Z) forms is however mitigated by a significant reduction in photoisomerization quantum yield (φ_{iso} below 0.1 for TPE-TPA derivatives). This so-called "amino conjugation effect" linked to the introduction of the TPA peripheral substituent, already observed for stilbene derivatives, is also observed in

two other AIE active stilbenoid derivatives studied in this work, namely **DPB-TPA** and **S-TPA** derivatives. All these observations demonstrate the overall effect of TPA substituents on the photochemistry AIE active stilbenoids. While providing new insights into the complex landscape of TPE derivatives excited state properties, we expect that these results will also drive the development of new photochromic compounds and molecular rotors based on the TPE core or others olefinic models. We are currently working on this topic.

Author Contributions

J.R.: Conceptualization, Formal analysis, Investigation, Methodology, Visualization, Writing – original draft, review and editing.

C.A.: Funding acquisition, Project administration, Writing-review and editing

C.M.: Conceptualization, Methodology, Project administration, Supervision, Writing – review and editing.

Conflicts of interest

There are no conflicts of interest to declare.

Data availability

The authors declare that the data supporting the findings of this study are available within the article and the Supplementary Information as well as from the authors upon reasonable request.

Acknowledgements

References

1   J. Wu, B. Yan, J. Meng, E. Yang, X. Ye and Q. Yao, Catalyst-free photo-reductions of aromatic olefins and carbonyl compounds, *Org. Biomol. Chem.*, 2022, **20**, 8638–8642.

2   A. B. Flynn and W. W. Ogilvie, Stereocontrolled Synthesis of Tetrasubstituted Olefins, *Chem. Rev.*, 2007, **107**, 4698–4745.

3   A. Ramani, B. Desai, B. Z. Dholakiya and T. Naveen, Recent advances in visible-light-mediated functionalization of olefins and alkynes using copper catalysts, *Chem. Commun.*, 2022, **58**, 7850–7873.

4   A. Del Vecchio, H. R. Smallman, J. Morvan, T. McBride, D. L. Browne and M. Mauduit, Challenges Arising from Continuous-Flow Olefin Metathesis, *Angew. Chem. Int. Ed.*, 2022, **61**, e202209564.

5   J. Corpas, P. Mauleón, R. Gómez Arrayás and J. C. Carretero, E/Z Photoisomerization of Olefins as an Emergent Strategy for the Control of Stereodivergence in Catalysis, *Adv. Synth. Catal.*, 2022, **364**, 1348–1370.

6   Tatsuo. Arai and Katsumi. Tokumaru, Photochemical one-way adiabatic isomerization of aromatic olefins, *Chem. Rev.*, 1993, **93**, 23–39.

7   T. Neveselý, M. Wienhold, J. J. Molloy and R. Gilmour, Advances in the E → Z Isomerization of Alkenes Using Small Molecule Photocatalysts, *Chem. Rev.*, 2022, **122**, 2650–2694.

8   D. H. Waldeck, Photoisomerization dynamics of stilbenes, *Chem. Rev.*, 1991, **91**, 415–436.

9   F. Würthner, Aggregation-Induced Emission (AIE): A Historical Perspective, *Angew. Chem. Int. Ed.*, 2020, **59**, 14192–14196.

10 Y. Xie and Z. Li, Recent Advances in the Z/E Isomers of Tetraphenylethene Derivatives: Stereoselective Synthesis, AIE Mechanism, Photophysical Properties, and Application as Chemical Probes, *Chem. – Asian J.*, 2019, **14**, 2524–2541.

11 Y. Huang, G. Zhang, R. Zhao and D. Zhang, Tetraphenylethene-Based cis/trans Isomers for Targeted Fluorescence Sensing and Biomedical Applications, *Chem. – Eur. J.*, 2023, **29**, e202300539.

12 K. Kokado and K. Sada, Consideration of Molecular Structure in the Excited State to Design New Luminogens with Aggregation-Induced Emission, *Angew. Chem. Int. Ed.*, 2019, **58**, 8632–8639.

13 K. Kokado, T. Machida, T. Iwasa, T. Taketsugu and K. Sada, Twist of C=C Bond Plays a Crucial Role in the Quenching of AIE-Active Tetraphenylethene Derivatives in Solution, *J. Phys. Chem. C*, 2018, **122**, 245–251.

14 D. D. La, S. V. Bhosale, L. A. Jones and S. V. Bhosale, Tetraphenylethylene-Based AIE-Active Probes for Sensing Applications, *ACS Appl. Mater. Interfaces*, 2018, **10**, 12189–12216.

15 Z. Yang, Z. Chi, Z. Mao, Y. Zhang, S. Liu, J. Zhao, M. P. Aldred and Z. Chi, Recent advances in mechano-responsive luminescence of tetraphenylethylene derivatives with aggregation-induced emission properties, *Mater. Chem. Front.*, 2018, **2**, 861–890.

16 Y. Cai, L. Du, K. Samedov, X. Gu, F. Qi, H. H. Y. Sung, B. O. Patrick, Z. Yan, X. Jiang, H. Zhang, J. W. Y. Lam, I. D. Williams, D. L. Phillips, A. Qin and B. Z. Tang, Deciphering the working mechanism of aggregation-induced emission of tetraphenylethylene derivatives by ultrafast spectroscopy, *Chem. Sci.*, 2018, **9**, 4662–4670.

17 J. Guan, R. Wei, A. Prlj, J. Peng, K.-H. Lin, J. Liu, H. Han, C. Corminboeuf, D. Zhao, Z. Yu and J. Zheng, Direct Observation of Aggregation-Induced Emission Mechanism, *Angew. Chem. Int. Ed.*, 2020, **59**, 14903–14909.

18 M. de la H. Tomás, M. Yamaguchi, B. Cohen, I. Hisaki and A. Douhal, Deciphering the ultrafast dynamics of a new tetraphenylethylene derivative in solutions: charge separation, phenyl ring rotation and C[double bond, length as m-dash]C bond twisting, *Phys. Chem. Chem. Phys.*, 2023, **25**, 1755–1767.

19 M. de la H. Tomás, M. Yamaguchi, B. Cohen, I. Hisaki and A. Douhal, Photocyclization reaction and

related photodynamics in the photoproducts of a tetraphenylethylene derivative with bulky substituents: unexpected solvent viscosity effect, *Phys. Chem. Chem. Phys.*, , DOI:10.1039/D3CP01295F.

20 J. Rouillon, C. Monnereau and C. Andraud, Reevaluating the Solution Photophysics of Tetraphenylethylene at the Origin of their Aggregation-Induced Emission Properties, *Chem. – Eur. J.*, 2021, **27**, 8003–8007.

21 J. Rouillon, C. Arnoux and C. Monnereau, Determination of Photoinduced Radical Generation Quantum Efficiencies by Combining Chemical Actinometry and 19F NMR Spectroscopy, *Anal. Chem.*, 2021, **93**, 2926–2932.

22 J.-S. Yang, S.-Y. Chiou and K.-L. Liau, Fluorescence Enhancement of trans-4-Aminostilbene by N-Phenyl Substitutions: The "Amino Conjugation Effect," *J. Am. Chem. Soc.*, 2002, **124**, 2518–2527.

23 L. Pfeifer, N. V. Hoang, S. Crespi, M. S. Pshenichnikov and B. L. Feringa, Dual-function artificial molecular motors performing rotation and photoluminescence, *Sci. Adv.*, 2022, **8**, eadd0410.

24 J. Rouillon, J. Blahut, M. Jean, M. Albalat, N. Vanthuyne, A. Lesage, L. M. A. Ali, K. Hadj-Kaddour, M. Onofre, M. Gary-Bobo, G. Micouin, A. Banyasz, T. Le Bahers, C. Andraud and C. Monnereau, Two-Photon Absorbing AIEgens: Influence of Stereoconfiguration on Their Crystallinity and Spectroscopic Properties and

Applications in Bioimaging, *ACS Appl. Mater. Interfaces*, 2020, **12**, 55157–55168.

25 J. Rouillon, L. M. A. Ali, K. Hadj-Kaddour, R. Marie-Luce, G. Simon, M. Onofre, S. Denis-Quanquin, M. Jean, M. Albalat, N. Vanthuyne, G. Micouin, A. Banyasz, M. Gary-Bobo, C. Monnereau and C. Andraud, Assembly of Aggregation-Induced Emission Active Bola-Amphiphilic Macromolecules into Luminescent Nanoparticles Optimized for Two-Photon Microscopy In Vivo, *Biomacromolecules*, 2022, **23**, 2485–2495.

26 Z. Zhang, W. Wang, M. O'Hagan, J. Dai, J. Zhang and H. Tian, Stepping Out of the Blue: From Visible to Near-IR Triggered Photoswitches, *Angew. Chem. Int. Ed.*, **n/a**, e202205758.

27 H. Goerner and D. Schulte-Frohlinde, Trans .fwdarw. cis photoisomerization of stilbene and 4-halogenated stilbenes, evidence for an upper excited triplet pathway, *J. Phys. Chem.*, 1979, **83**, 3107–3118.

28 J. L. Charlton and J. Saltiel, An analysis of trans-stilbene fluorescence quantum yields and lifetimes, *J. Phys. Chem.*, 1977, **81**, 1940–1944.

Supplementary Information

Modulation of the photochromic properties of TPE and other tetrasubstituted olefins by the "amino conjugation effect": a quantitative study

Jean Rouillon,[*a,b] Chantal Andraud[a] and Cyrille Monnereau[a]

a/ Univ Lyon, Ecole Normale Supérieure de Lyon, Laboratoire de Chimie, CNRS UMR 5182, 69342 Lyon, France
b/ Department of Chemistry and Chemical Engineering, Chalmers University of Technology, Kemigården 4, 412 96 Göteborg, Sweden.

Synthesis

Synthesis of **TPE-TPA**, **DPB-TPA** and **S-TPA** were already depicted in reference [1].

Photoisomerization quantum yield determination

a) For **TPE-TPA** and **DPB-TPA**:

- ^{1}H NMR spectra were recorded at room temperature on a Bruker Avance 400 spectrometer operating at 400 MHz. $CDCl_3$ (d, 99.8%) was purchased from Euroisotop. Chemical shifts are given as values (ppm) referenced to the peak of $CDCl_3$ (7.26 ppm). All experiments were performed in quartz NMR tubes. The accuracy of the NMR integrations in the titration conditions was checked by comparing the integrations obtained on a test sample acquired with a relaxation time T1 corresponding to those used in the standard titration experiments, T1 being acquired with approximately five times longer relaxation delays. The measured integrations remained unchanged. NMR integrations and peak heights were estimated using MestReNova. Exponential fitting, tangent and exact method treatment of the obtained data were performed using Origin software.

- The irradiation source was the 450 W xenon arc lamp of a Horiba Jobin-Yvon Fluorolog-3 spectrofluorimeter, and the irradiation wavelength was selected using an iHR320 excitation monochromator with 1200 groves.mm^{-1} grating. Irradiation experiments were performed in a calibrated integrative sphere (2π steradian covered with spectralon®, model G8 from GMP). The value of incident photon flux used were determined by chemical actinometry based on the photoconversion of 2-nitrobenzaldehyde to 2-nitrosobenzoic acid.[2] Values obtained accordingly are given in Table S1.

Table S1. Light intensities and maximum wavelength used for irradiation of **TPE-TPA** and **DPB-TPA**.

	TPE-TPA	DPB-TPA
I_0 (s^{-1})	9.48 x 10^{15}	1.18 x 10^{16}
λ (nm)	372	358

- The irradiation of NMR tube in an integrating sphere is fully described in a previous paper.[2] The accuracy of the method was verified by comparing this setup with conventional irradiation in a spectroscopic cuvette under constant agitation, with deviations in incident power measurements of less than 3%. The ratio of photons absorbed by the contents of the NMR tube in the integration sphere to the incident photon flux was estimated by integrating the excitation spectra of the lamp in the absence and presence of the sample. Stock solutions in $CDCl_3$ were prepared at specific concentrations using volumetric flasks. The solutions were transferred to the NMR tube. Irradiation was started at t = 0, ^{1}H spectra were recorded at precise intervals of irradiation time and the conversion was calculated from the respective integrations of reactant and product(s). For **TPE-TPA** isomers, the center of the multiplet at 7.13 ppm was chosen to follow the evolution of the proportion of E isomer and the center of the multiplet at 7.11 ppm for the Z isomer. In the case of **DPB-TPA**, the concentrations were determined from the relative heights of the peaks at 7.37 ppm for the E isomer and 7.31 ppm for the Z isomer.

- Two methodologies were employed to determine the photoisomerization quantum yields φ$_{iso}$ (Photoisomerization of the (Z)-isomer has been chosen for illustration in the following formula; similar logic applies to the (E)-isomer).

(i) Extrapolation method: the kinetic constant k$_{iso}$ associated to the (Z) → (E) photoisomerization is estimated at the beginning of the reaction at t = 0.[3] At this stage, the (E)-isomer being in negligible concentration in the reaction mixture, the constant k$_{iso}$ can be readily obtained according to equation S1:

$$\lim_{([Z]-[Z]_0) \to 0} \frac{[Z]_0-[Z]}{t} = k_{iso} \quad \text{(S1)}$$

Photoisomerization quantum yield can be derived from the measured k$_{iso}$ according to equation S2:

$$\Phi_{iso} = \frac{k_{iso}.N_A.V}{I_{abs}} \quad \text{(S2)}$$

With k$_{iso}$ is the kinetic constant of the photoisomerization (mol.L^{-1} .s^{-1}), N_A, the Avogadro constant, V, the volume of the solution (L), and I$_{abs}$, the absorbed photon flux (s^{-1}). Real amount I$_{abs}$ of photon flux absorbed by the NMR tube in the integration sphere can be calculated following equation:

$$I_{abs} = I_0 \left(1 - \frac{L_c}{L_a} \right) \quad \text{(S3)}$$

With I_0 corresponds to the incident photon flux, L_c and L_a are the integrated excitation spectra of the sphere (i.e. measured signal of the light source) with and without the sample NMR tube respectively.

(ii) Exact method: this consists in obtaining a pair of solutions to the differential equation S4, describing the entire process of photoisomerization [4] by using regression algorithms applied to non-linear multivariate functions. Bayda *et al.* propose to apply the Levenberg-Marquardt algorithm to an exponential form of the solution:[4]

$$exp\left(-\frac{t}{s}\right) = exp\left(\frac{\varepsilon_Z - \varepsilon_E}{I_{abs}(z+e)}\frac{[Z]-[Z]_0}{s}\right) \times \left(1 + \frac{1}{[Z]_0}\left(1 + \frac{e}{z}\right)([Z]-[Z]_0)\right)^{\frac{[Z]_0}{s}\frac{z\varepsilon_E + e\varepsilon_Z}{I_{abs}(z+e)^2}} \quad \text{(S4)}$$

With $[Z]_0$, the initial concentration of the (Z)-isomer, $z = \varepsilon_Z\Phi_{Z\to E}$, $e = \varepsilon_E\Phi_{E\to Z}$, and s, a scale factor.

By applying the fitting algorithm to the curve of exp(- ts) versus $[Z] - [Z]_0$ (equation S4), a pair of solutions (z,e) is calculated. This method thus makes it possible to obtain the two quantum yields of photoisomerization with the study of a single kinetic and by applying it to the whole reaction.

Parameters and quantum yields deduced by both methods are summarized in Table S2. For photoisomerization kinetics, χ^2 test of the exponential fit with the constant k_{iso} extrapolated from the tangent at zero-time are presented. For the exact method, χ^2 test of the fit to equation S4 with the obtained photoisomerization quantum yield Φ_1 and Φ_2 are included in the corresponding graphs. In all cases, good consistencies were found when comparing the yields obtained by both methods.

Table S2. Summary of the parameters and yields of photoisomerization obtained for **TPE-TPA** and **DPB-TPA**.

	(Z)-TPE-TPA	(E)-TPE-TPA	(Z)-DPB-TPA	(E)-DPB-TPA
k_{iso} (mol.L^{-1}.s^{-1})	2.33×10^{-6}	1.98×10^{-6}	1.82×10^{-6}	1.16×10^{-6}
V (L)	5.00×10^{-4}	5.00×10^{-4}	5.00×10^{-4}	5.00×10^{-4}
L_a	6.85×10^{7}	6.72×10^{7}	6.45×10^{7}	3.72×10^{7}
L_c	1.36×10^{6}	1.25×10^{6}	1.16×10^{6}	4.02×10^{6}
$1-(L_c/L_a)$	0.802	0.812	0.821	0.892
Φ_{iso} (extrapolation)	0.09	0.08	0.06	0.04
χ^2 (extrapolation)	0.984	0.999	0.999	0.998
Φ_{iso} (exact method)	0.10	0.08	0.06	0.04
χ^2 (exact method)	0.965	0.998	0.990	0.983

b) For **S-TPA**,

Since the stilbene derivative **S-TPA** has more pronounced spectral signatures changes between the (E) and (Z) isomers than **TPE-TPA** and **DPB-TPA**, it was decided to monitor photoisomerization by successive absorption spectra.
The sample was placed in a cuvette equipped with a magnetic stirrer. The light intensity was determined using a power-meter from Starlite Ophir. Absorption spectra were recorded every minute using a Cary50 UV-vis spectrometer, under constant mixing.
Solution has been prepared in CDCl$_3$ to give an absorbance of approx. A = 1 (i.e. total absorption regime). At longer irradiation times, photocyclization could no longer be neglected. Therefore, the linear fit to extrapolate k_{iso} was performed when the E isomer (non-photocyclizable) was still predominant.
The φ_{iso} yield was therefore determined using the extrapolation method (measurement of $\left(\frac{dA}{dt}\right)_0$) :

$$\phi_{iso} = \frac{\left(\frac{dA}{dt}\right)_0 . C_0 . N_a . V}{I_0 . A_0} \quad \text{(S5)}$$

Parameters and quantum yields deduced are summarized in Table S3.

Table S3. Summary of the parameters and yields of photoisomerization obtained for **S-TPA**.

	(E)-S-TPA
dA/dt	0,075
C_0 (mol.L^{-1}.s^{-1})	3.0 x 10^{-5}
V (L)	0.002
I_0 (s^{-1})	1.30 x 10^{16}
A_0	1.17
Φ_{iso} (extrapolation)	0.18
χ^2 (extrapolation)	0.990
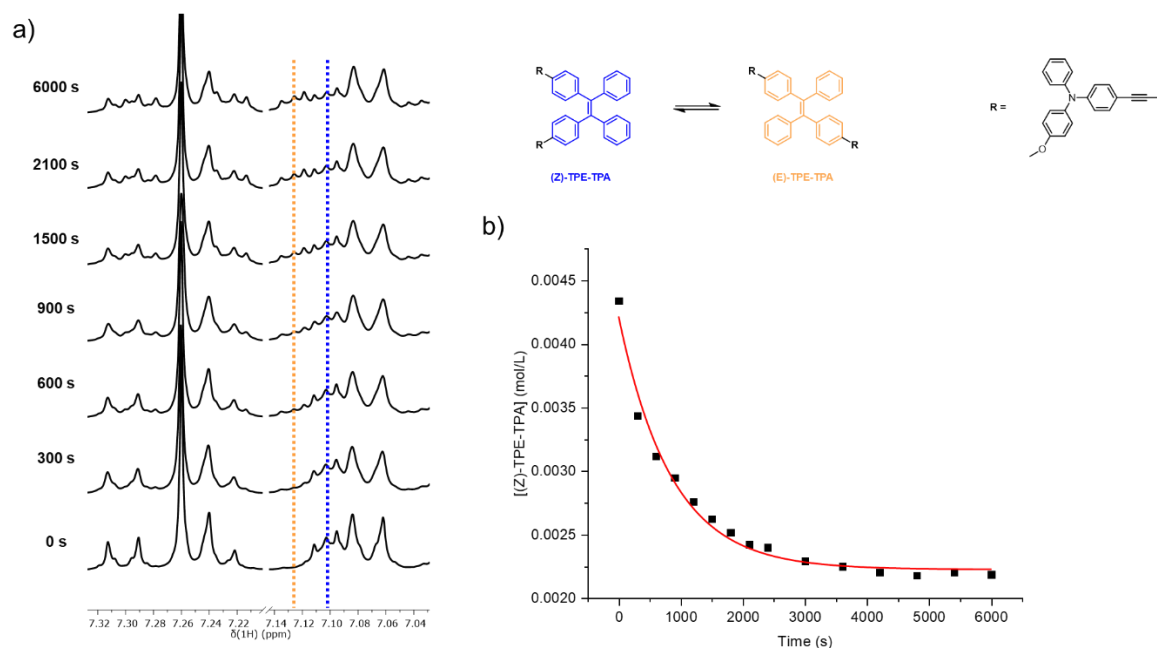
Fig. S1 (a) Close-up view on aromatic region of ^{1}H NMR spectra during irradiation of **(Z)-TPE-TPA** (in solution of CDCl$_3$, at room temperature, with a spectrometer operating at 400 MHz). (b) Photoisomerization kinetic of **(Z)-TPE-TPA** in solution (Red curve corresponding to exponential fit).
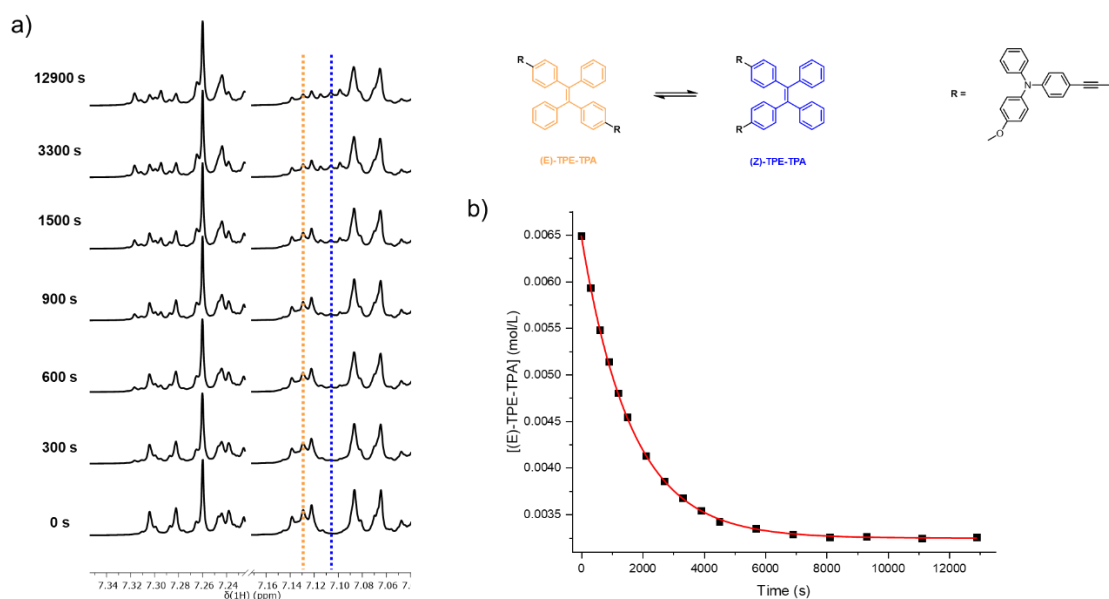
Fig. S2 (a) Close-up view on aromatic region of ^{1}H NMR spectra during irradiation of **(E)-TPE-TPA** (in solution of CDCl$_3$, at room temperature, with a spectrometer operating at 400 MHz). (b) Photoisomerization kinetic of **(E)-TPE-TPA** in solution (Red curve corresponding to exponential fit).
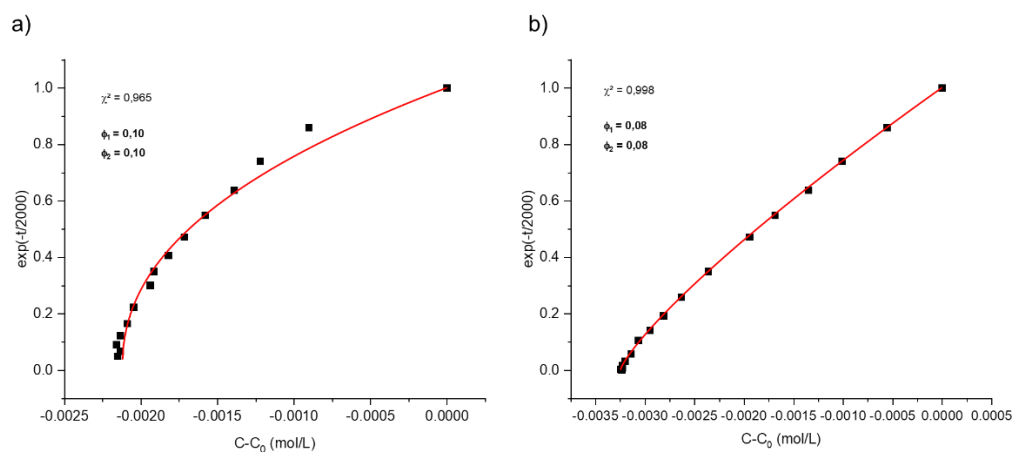
Fig. S3 Exact method treatment of photoisomerization kinetics of (a) **(Z)-TPE-TPA** and (b) **(E)-TPE-TPA** (Red curve corresponding to the fit to equation S4).

Fig. S4 (a) Close-up view on aromatic region of ^{1}H NMR spectra during irradiation of **(Z)-DPB-TPA** (in solution of CDCl$_3$, at room temperature, with a spectrometer operating at 400 MHz). (b) Photoisomerization kinetic of **(Z)-DPB-TPA** in solution (Red curve corresponding to exponential fit).

Fig. S5 (a) Close-up view on aromatic region of ^1H NMR spectra during irradiation of **(E)-DPB-TPA** (in solution of $CDCl_3$, at room temperature, with a spectrometer operating at 400 MHz). (b) Photoisomerization kinetic of **(Z)-DPB-TPA** in solution (Red curve corresponding to exponential fit).

Fig. S6. Exact method treatment of photoisomerization kinetics of (a) **(Z)-DPB-TPA** and (b) **(E)-DPB-TPA** (Red curve corresponding to the fit to equation S4).
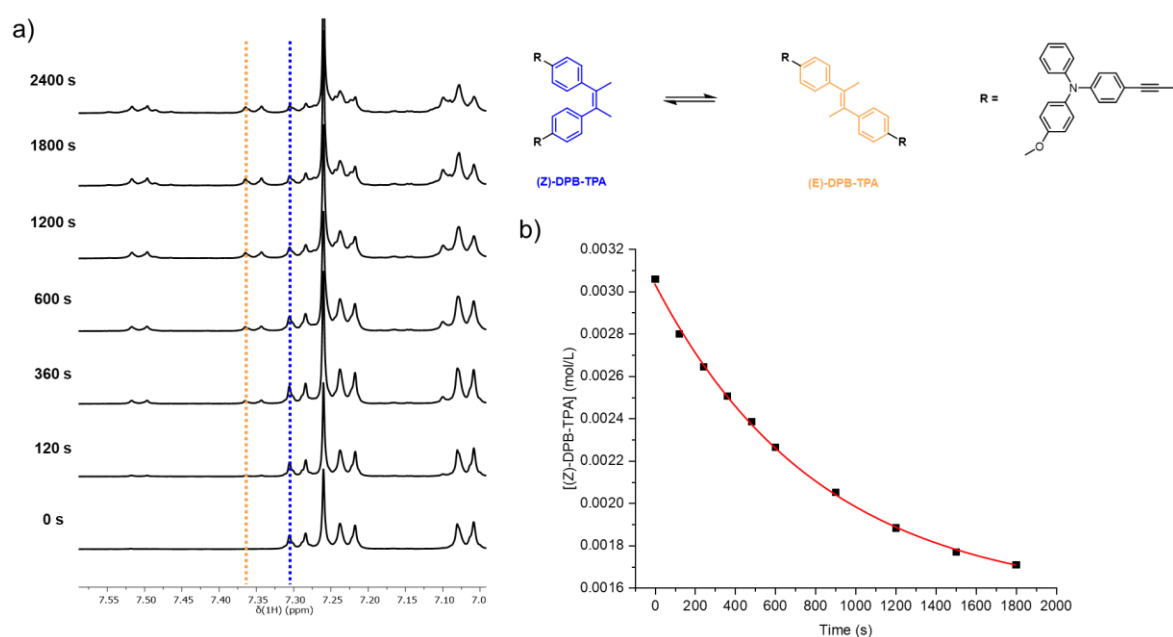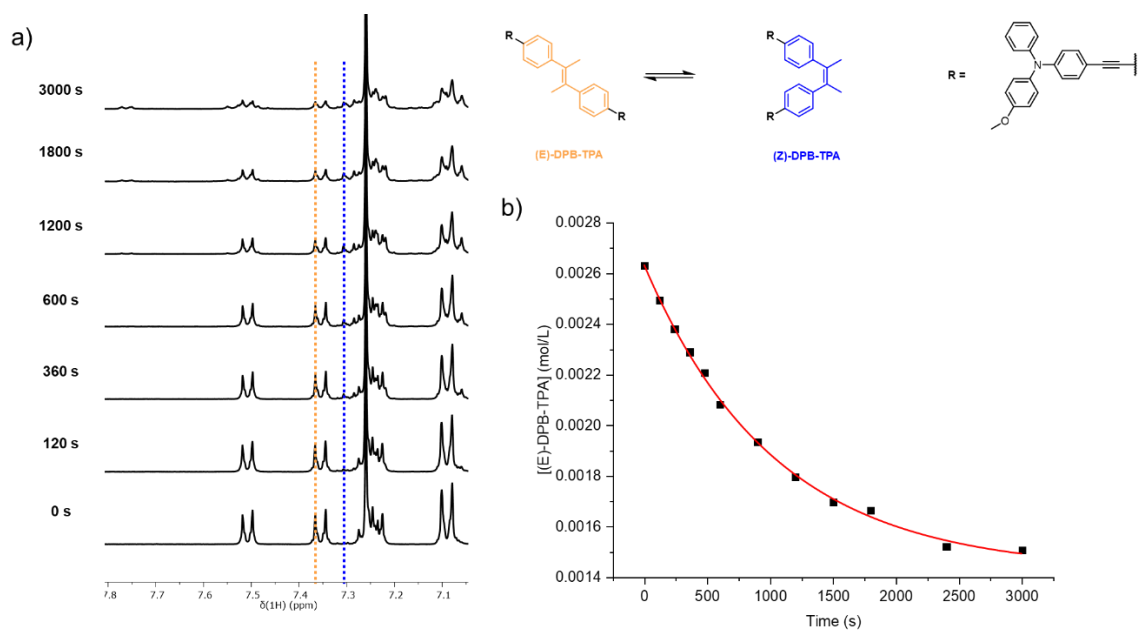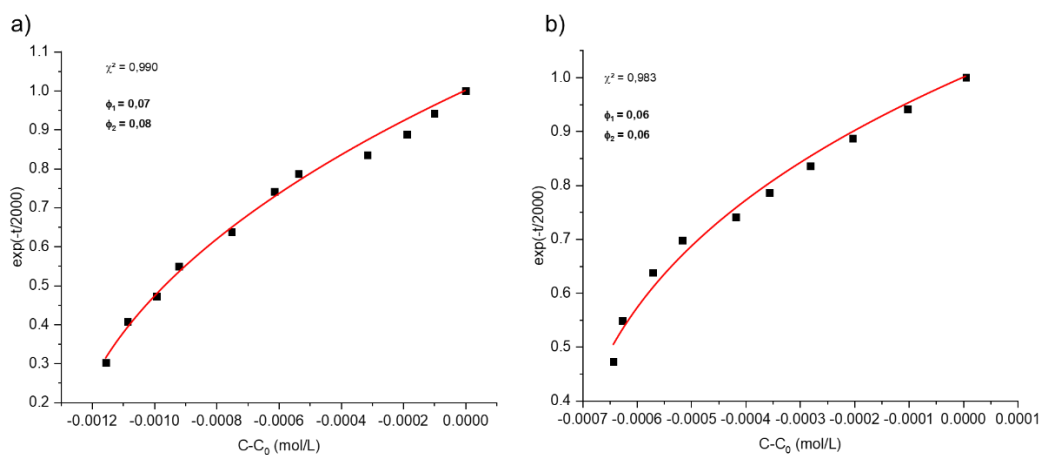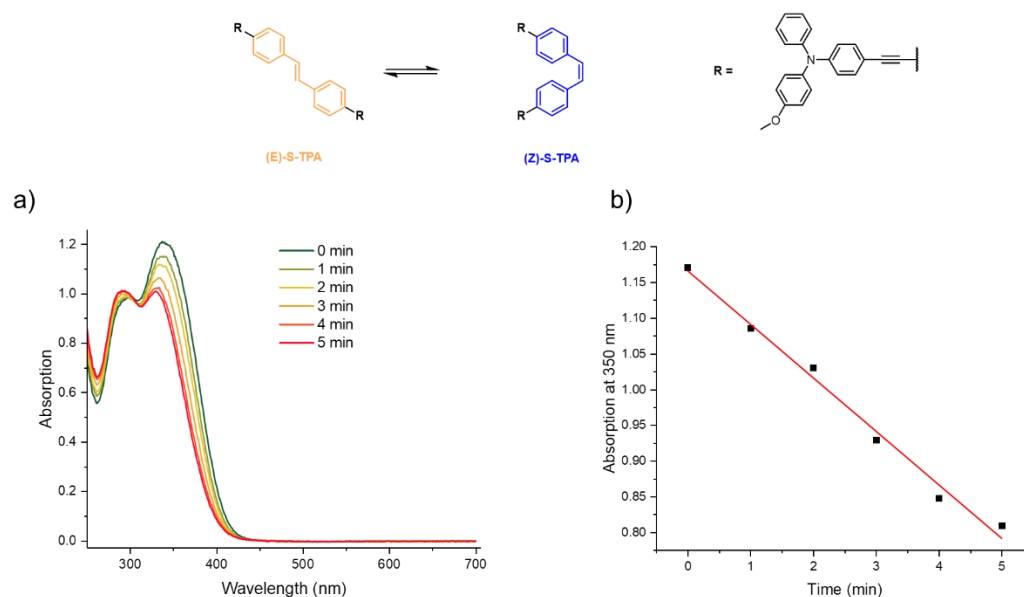
Fig. S7 (a) Absorption spectra during irradiation of **(E)-S-TPA** (1 minute interval between each spectra, in solution of CDCl$_3$, at room temperature). (b) Photoisomerization kinetic of **(E)-S-TPA** in solution (Red curve corresponding to linear fit).

Table S4. Ratios of **(Z)-TPE-TPA** calculated by RMN-^{1}H during irradiation

Time (s)	Intensity (a.u.)		(Z)-isomer ratio
	(E)-Peak	**(Z)-Peak**	
0	-	-	1.000
300	128.2	589.4	0.792
600	170.4	526.1	0.719
900	198.7	508.9	0.679
1200	242.4	512.1	0.636
1500	264.6	489.1	0.604
1800	284.9	477.2	0.581
2100	309	472.7	0.558
2400	297.5	445.2	0.553
3000	335.5	454.6	0.528
3600	336.3	438.1	0.519
4200	346.6	433	0.508
4800	363.1	443.7	0.503
5400	328	409.3	0.508
6000	340.2	418.1	0.504

Table S5. Ratios of **(E)-TPE-TPA** calculated by RMN-^{1}H during irradiation.

Time (s)	Intensity (a.u.)		(E)-isomer ratio
	(E)-Peak	**(Z)-Peak**	
0	-	-	1.000
300	1000	183.7	0.914
600	928.9	262.1	0.844
900	887.1	325.4	0.792
1200	806.2	373.1	0.740
1500	781.1	426.4	0.700
2100	693.9	487.2	0.636
2700	639.3	524.7	0.594
3300	626.4	570.8	0.566
3900	596.4	587.2	0.545
4500	545.3	574.3	0.527
5700	566	620.8	0.516
6900	538.7	612.8	0.506
8100	526.9	608.9	0.502
9300	540.7	623.3	0.503
11100	536.4	624.3	0.500
12900	544.4	630.4	0.502

Table S6. Ratios of **(Z)-DPB-TPA** calculated by RMN-^{1}H during irradiation.

Time (s)	Intensity (a.u.)		(Z)-isomer ratio
	(E)-Peak	(Z)-Peak	
0	-	-	1.000
120	65	816.7	0.915
240	98.9	735.6	0.864
360	129.2	682.5	0.819
480	154.7	638.8	0.780
600	162.4	540.4	0.740
900	205.5	487.7	0.670
1200	218.2	408	0.616
1500	251.7	403.5	0.579
1800	250.2	370.3	0.559
2400	244.1	282.9	0.498

Table S7. Ratios of **(E)-DPB-TPA** calculated by RMN-^{1}H during irradiation.

Time (s)	Intensity (a.u.)		(E)-isomer ratio
	(Z)-Peak	(E)-Peak	
0	-	-	1.000
120	65	816.7	0.915
240	98.9	735.6	0.864
360	129.2	682.5	0.819
480	154.7	638.8	0.780
600	162.4	540.4	0.740
900	205.5	487.7	0.670
1200	218.2	408	0.616
1500	251.7	403.5	0.579
1800	250.2	370.3	0.559
2400	244.1	282.9	0.498

Comparison of the spectroscopic properties of the E and Z forms of other stereopure TPE derivatives reported in previous literature, and associated references.
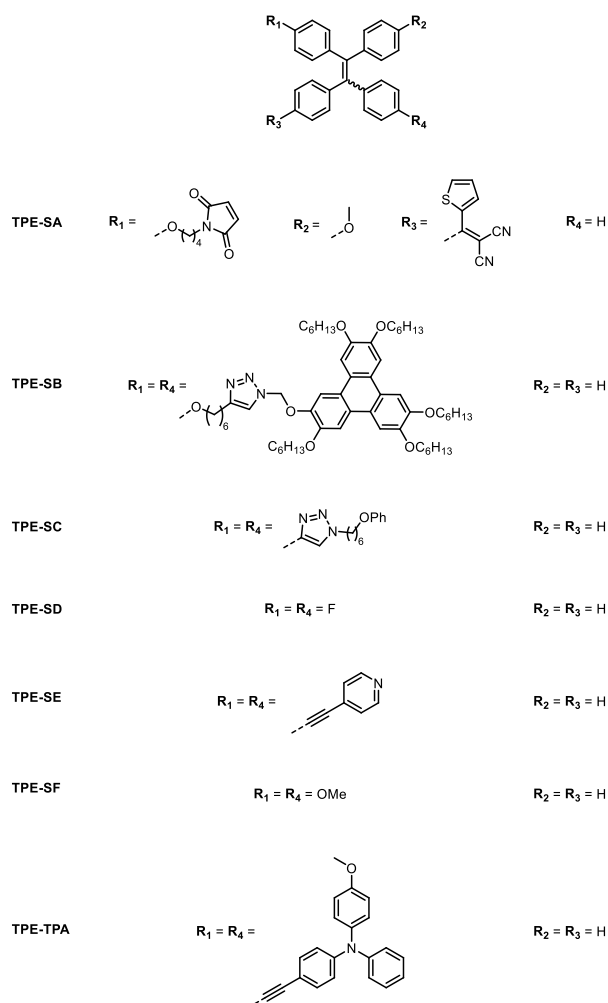
TPE-SA $R_1 =$ (structure) $R_2 =$ (structure) $R_3 =$ (structure) $R_4 =$ H

TPE-SB $R_1 = R_4 =$ (structure) $R_2 = R_3 =$ H

TPE-SC $R_1 = R_4 =$ (structure) $R_2 = R_3 =$ H

TPE-SD $R_1 = R_4 =$ F $R_2 = R_3 =$ H

TPE-SE $R_1 = R_4 =$ (structure) $R_2 = R_3 =$ H

TPE-SF $R_1 = R_4 =$ OMe $R_2 = R_3 =$ H

TPE-TPA $R_1 = R_4 =$ (structure) $R_2 = R_3 =$ H

Table S8. Absorption differences between (E) and (Z) isomers of stereopures TPE derivatives already described in the literature (only some illustrating examples in case of no spectral differences).

Compound	Absorption of (E)-isomer (nm)	Absorption of (Z)-isomer (nm)	Shift absorption E-Z (cm^{-1})	Solvent	Ref.
TPE-SA	440	440	0	DMSO	[5]
TPE-SB	290	290	0	THF	[6]
TPE-SC	332	332	0	THF	[7]
TPE-SD	304	305	108	THF	[8]
TPE-SE	345	347	167	EtOH	[9]
TPE-SF	322	320	194	THF	[8]
TPE-TPA	370	361	674	THF	[1]

References

1 J. Rouillon, J. Blahut, M. Jean, M. Albalat, N. Vanthuyne, A. Lesage, L. M. A. Ali, K. Hadj-Kaddour, M. Onofre, M. Gary-Bobo, G. Micouin, A. Banyasz, T. Le Bahers, C. Andraud and C. Monnereau, Two-Photon Absorbing AIEgens: Influence of Stereoconfiguration on Their Crystallinity and Spectroscopic Properties and Applications in Bioimaging, *ACS Appl. Mater. Interfaces*, 2020, **12**, 55157–55168.

2 J. Rouillon, C. Arnoux and C. Monnereau, Determination of Photoinduced Radical Generation Quantum Efficiencies by Combining Chemical Actinometry and 19F NMR Spectroscopy, *Anal. Chem.*, 2021, **93**, 2926–2932.

3 J. M. Donahue and W. H. Waddell, The Trans → Cis Photoisomerization of Protonated Retinyl Schiff Bases, *Photochem. Photobiol.*, 1984, **40**, 399–401.

4 M. Bayda, G. L. Hug, J. Lukaszewicz, M. Majchrzak, B. Marciniec and B. Marciniak, Kinetics of reversible photoisomerization: determination of the primary quantum yields for the E–Z photoisomerization of silylenephenylenevinylene derivatives, *Photochem. Photobiol. Sci.*, 2009, **8**, 1667–1675.

5 C.-J. Zhang, G. Feng, S. Xu, Z. Zhu, X. Lu, J. Wu and B. Liu, Structure-Dependent cis/trans Isomerization of Tetraphenylethene Derivatives: Consequences for Aggregation-Induced Emission, *Angew. Chem. Int. Ed.*, 2016, **55**, 6192–6196.

6 W.-H. Yu, C. Chen, P. Hu, B.-Q. Wang, C. Redshaw and K.-Q. Zhao, Tetraphenylethene–triphenylene oligomers with an aggregation-induced emission effect and discotic columnar mesophase, *RSC Adv.*, 2013, **3**, 14099–14105.

7 J. Wang, J. Mei, R. Hu, J. Z. Sun, A. Qin and B. Z. Tang, Click Synthesis, Aggregation-Induced Emission, E/Z Isomerization, Self-Organization, and Multiple Chromisms of Pure Stereoisomers of a Tetraphenylethene-Cored Luminogen, *J. Am. Chem. Soc.*, 2012, **134**, 9956–9966.

8 K. Kokado, T. Machida, T. Iwasa, T. Taketsugu and K. Sada, Twist of C═C Bond Plays a Crucial Role in the Quenching of AIE-Active Tetraphenylethene Derivatives in Solution, *J. Phys. Chem. C*, 2018, **122**, 245–251.

9 Z. Wang, X. Cheng, A. Qin, H. Zhang, J. Z. Sun and B. Z. Tang, Multiple Stimuli Responses of Stereo-Isomers of AIE-Active Ethynylene-Bridged and Pyridyl-Modified Tetraphenylethene, *J. Phys. Chem. B*, 2018, **122**, 2165–2176.